

# Efficient computation of baryon interpolating fields in Lattice QCD

Eloy Romero<sup>1,\*</sup> and Kostas Orginos<sup>2,3,\*\*</sup>

<sup>1</sup>Department of Computer Science, The College of William & Mary, USA

<sup>2</sup>Department of Physics, The College of William & Mary, USA

<sup>3</sup>Jefferson Laboratory, USA

**Abstract.** In this work we present an efficient construction of baryon interpolating fields for lattice QCD computations of two and three point functions. These are essential building blocks of computations of nucleon parton distribution functions (PDFs), generalized parton distribution functions (GPDs) and transverse momentum dependent distributions functions (TMDs). Lattice QCD computations of these quantities can provide additional input to assist with the global fits on experimental data for determining TMDs, GPDs and PDFs.

A vital component of our long term project of determining hadronic structure from lattice QCD is the ability to compute a large class of matrix elements with high precision, both statistical and systematic. To that extent, we plan to capitalize on distillation [1], for constructing suitable interpolating fields for the nucleon that has already been very successful in spectroscopy computations.

The basic idea of distillation is to restrict the operators to a small subspace (the distillation basis) containing substantial contributions of the relevant eigenstates. The reduction in the rank of the operators dramatically cuts down the cost of computing all elements of the propagation matrix, allowing for measuring more complex hadron correlation functions.

Still, the amount of computation and storage overgrows with the lattice size  $N$  and the rank of the distillation basis,  $n$ . The optimal rank of the distillation basis is determinate experimentally, but it is roughly proportional to the volume of the spatial dimensions of the lattice. We give an idea of the costs by showing the amount of floating-point operations and the footprint memory requirements in big-O notation considering a 4D lattice that all dimension have equal size in which the volume of the spatial dimensions is proportional to the distillation basis rank,  $n$ . In these terms, the most expensive parts of the computations are the formation of the matrix elements, which are tensors generated from contracting matrices (basis), requiring roughly  $n^{3.3}$  operations for mesons (two matrices are contracted) and  $n^{4.3}$  for baryons (three matrices are contracted). The perambulators are square matrices generated by projecting the inverse of the Dirac operator and require  $n^{2.3}$  operations. At the final step of the computation, matrix elements and perambulators are contracted together and that requires  $n^3$  and  $n^4$  operations for mesons and baryons respectively. Table 1 details the time that each task takes for baryons in the example used along within this document.

In this project, we focus on accelerating the generation of baryon elementals, whose time dominates over the rest of the tasks. Despite the apparent simplicity of tensor contractions,

---

\*e-mail: eloy@cs.wm.edu

\*\*e-mail: knorgi@wm.edu

**Table 1.** Asymptotic computational cost, reference time per configuration and time-slice source, and software involved in the time-consuming tasks in estimating the two point correlation functions for a lattice  $32^3 \times 64$  in a single femto[4]’s node.

Computation	Operations cost	Memory footprint	Example time	Main libraries
Distillation basis	$n^{2.3}$	$n^{2.3}$	0.1 h	PRIMME
Baryon elementals	$n^{4.3}$	$n^{3.3}$	16 h	Harom
Perambulators	$100n^{2.3}$	$100n^{2.3}$	3 h	Chroma, Qphix/mg_proto
Contractions	$n^4$	$n^{3.3}$	0.1 h	Hadron, tensor

developing high-performance implementations is challenging, and the efforts have to be specialized for the characteristics of the tensors and the computing device. Unlike the multiplication of matrices, few libraries, such as CFT[2] and libtensor[3], provide a powerful and flexible way to specify the tensor contractions if one is willing to sacrifice some performance.

The first optimization that we propose does not reduce the number of operations, but instead reorder the operations to minimize memory requests and operands dependency, increasing the utilization of the many arithmetic-logic units available on modern CPUs. By relying on high-performance implementations of matrix-matrix multiplication, we take advantage of optimizations specific to the computing device and the dimensions of the tensors already available in these libraries. The second approach addresses not only the computational time but also the demanding I/O requirements of the calculation. We have explored a technique that finds a sparse approximate representation of the distillation basis in a way that the baryon elementals are also sparse.

### BLAS acceleration of baryon elementals

To explain the caveats of the approach, we introduce a simplified description of the actual tensor contractions that correspond to the computation of the baryon elementals for a particular time-slice, gauge configuration, and displacements combination. The operands of the contraction include

- three 5D tensors (which can be the distillation basis or an operator acting on the basis),  $\mathbf{v}$ ,  $\mathbf{w}$ ,  $\mathbf{y}$ , with components on the 3D space lattice  $L_N$  of dimension  $N$ , the three color space components  $C = 1, 2, 3$ , and the last index is the distillation basis column from 1 to  $n$ ;
- a 4D tensor  $\mathbf{z}$  (which is a phase,  $z^{(\mathbf{x},l)} = e^{-i\mathbf{p}\cdot\mathbf{x}}$ ), which also has components on  $L_N$  and an index for the momenta; and finally,
- the color contraction is indicated with  $\epsilon$ , which is a sparse, antisymmetric tensor representing the color contraction,  $\epsilon^{(1,2,3)} = 1$ , and  $\epsilon^{(\alpha,\alpha,\beta)} = 0$ ,  $\epsilon^{(\alpha,\beta,\gamma)} = -\epsilon^{(\beta,\alpha,\gamma)} = -\epsilon^{(\alpha,\gamma,\beta)}$ .

The tensors are operated as follows:

$$B^{(i,j,k,l)} = \sum_{\mathbf{x} \in L_N, \alpha, \beta, \gamma \in C} \epsilon^{(\alpha,\beta,\gamma)} v^{(\mathbf{x},\alpha,i)} w^{(\mathbf{x},\beta,j)} y^{(\mathbf{x},\gamma,k)} z^{(\mathbf{x},l)}, \quad \text{for } 1 \leq i, j, k \leq n, 1 \leq l \leq M. \quad (1)$$

We studied all alternatives for implementing the tensor contraction Eq. (1) by grouping the operands into two groups. Table 2 shows all the relevant possibilities. For instance, creating the tensor with  $\epsilon$ ,  $\mathbf{v}$ ,  $\mathbf{w}$ , and  $\mathbf{y}$  and then contracted with  $\mathbf{z}$  requires the minimum number of floating-point operations. However, its performance is bounded by the memory bandwidth of the computing node. In modern CPUs with many arithmetic-logic units, the grouping with better performance, despite doing three times more floating-point operations

**Table 2.** Asymptotic extra auxiliary memory and floating-point operations (FLOPs) in computing the tensor contraction at Eq. (1) depending on how the operands are grouped, for a lattice of volume  $N^3$ , and basis  $\mathbf{v}$ ,  $\mathbf{w}$ ,  $\mathbf{y}$  of rank  $n$ , and basis  $\mathbf{z}$  of rank  $M$ .

Grouping	Aux. memory	FLOPs
$\epsilon v w y z$	0	$9 M n^3 N^3$
$(\epsilon v)(w y z)$	$6 M n^2 N^3$	$6 M n^3 N^3$
$(\epsilon v w)(y z)$	$3 n^2 N^3$	$3 M n^3 N^3$
$(\epsilon v w y)(z)$	$n^3 N^3$	$M n^3 N^3$

**Table 3.** Performance comparison in time floating-point operations per seconds (GFLOPS) of the original version (Grouping  $(\epsilon v w y)(z)$ ) and the new implementation (Grouping  $(\epsilon v w)(y z)$ ) in computing the baryon elementals for a configuration with a lattice  $32^3 \times 64$ , 19 momenta, and 18 displacements on a femto’s node. Reported times do not include reading/writing disk operations. Maximum peak performance for a femto’s node is 1800 GFLOPS, and bounded by memory bandwidth is 40 GFLOPS.

$n$	Grouping $(\epsilon v w y)(z)$		Grouping $(\epsilon v w)(y z)$	
	Time (s)	GFLOPS	Time (s)	GFLOPS
32	4,923	38	529	1,066
64	33,191	45	4,048	1,115
128	–	–	29,219	1,235
256	–	–	162,542	1,776

than the previous variant, contracts the auxiliary tensor  $\mathbf{f}$ , formed with  $\epsilon$ ,  $\mathbf{v}$ , and  $\mathbf{w}$ , with the tensor  $\mathbf{g}$ , formed with  $\mathbf{y}$  and  $\mathbf{z}$ .

For contracting the tensors  $\mathbf{f}$  and  $\mathbf{g}$ , we propose to bypass most of the effort of developing and maintaining a high-performance tensor contraction by relying on optimized BLAS libraries for computing matrix-matrix multiplications, such as OpenBLAS and MKL. The use of BLAS is a state-of-the-art practice in tensor contraction on CPUs[5] and GPUs[6].

We developed the implementation inside the library `harom`<sup>1</sup>, which is part of the software suite for spectroscopy at Jefferson Laboratory. Like the rest of the `harom`’s code, our implementation supports shared memory (with OpenMP) and distributed memory (with MPI) paradigms. In `harom`, the lattice dimensions of the operands are distributed among the processes. So our code first contracts the local part of the basis  $\mathbf{v}$ ,  $\mathbf{w}$ ,  $\mathbf{y}$ , and  $\mathbf{z}$ , and, in the end, a single global reduction adds the partial results at every process. If threading is used, the threads independently work on different partitions of the  $i, j$  indices of the baryon elemental.

We have tested the performance of the new implementation mostly on Intel Skylake and Phi processors. The results show that the new implementation is ten times faster on average than the original code in computing the baryon elementals. On Tab. 3, we report the results on femto [4], a cluster at The Collage of William & Mary. As the range of the distillation basis increases, the overheads of copying back and forth from the `harom` representation of the tensors to the formats imposed by BLAS diminishes, and the performance of the new implementation gets closer to the peak performance of the node.

A new bottleneck has appeared after the drastic reduction in computing the baryon elementals: the time for writing the baryon elementals on the global file systems starts to dominate. For a distillation basis with a  $n = 256$  rank, the time that takes writing the baryon elementals on disk is double that the time expended in computing them. The approach that

<sup>1</sup><https://github.com/JeffersonLab/harom>

we introduce in the following aims at reducing not only the computational time but also the storage of the baryon elementals.

### Blocked distillation basis

The distillation basis consists of the eigenvectors from the lower part of the spectrum of a Laplacian-like operator  $\nabla^2$ ,

$$\nabla^{2(x,y)} = 6\delta_{x,y} - \sum_{\mathbf{j} \in \{(1,0,0), (0,1,0), (0,0,1)\}} U_{\mathbf{j}}^{(x)} \delta_{x+\mathbf{j},y} + U_{\mathbf{j}}^{(x-\mathbf{j})\dagger} \delta_{x-\mathbf{j},y},$$

where  $U$  is the gauge field restricted to a particular time-slice that may have been smeared, which is not relevant in this context. Like the eigenvectors of the Laplacian, those eigenvectors have common components on the local scale [7]. The use of a local support basis to approximate the lower spectrum is a critical ingredient in the construction of the prolongator and restrictor operators in multigrid [8, 9]. Also, it has been used to compress the eigenvectors [10].

The baryon elementals generated from this local-supported, sparse bases can be computed faster, and the resulting tensors are sparse also. These sparse tensors are faster to write on disk and to contract together with other tensors.

The new approach for generating the distillation basis of rank  $n$  in a time-slice is as following. First, we divide the lattice in  $d$  equally sized domains and restrict  $f(\nabla^2)$  to each of the domains, where  $f$  is function on  $\mathfrak{X}$  whose output is non-negative real numbers. The new basis is composed by taken  $n/d$  eigenvectors from each subdomain with the largest eigenvalues. The function  $f$  controls the weight of the eigenvectors. For instance, if  $f$  is constant, all eigenvectors matter equally.

We avoid the evaluation of  $f(\nabla^2)$  by working with a truncated approximate eigendecomposition of  $f(\nabla^2)$ ,  $f(\nabla^2)V = V\Lambda$ . Then the eigendecomposition of  $Vf(\nabla^2)V^\dagger$  restricted to each subdomain  $s$ ,  $V^{s\dagger}f(\Lambda)V^s W^s = W^s \tilde{\Lambda}^s$  is related to the singular value decomposition of  $V^s f(\Lambda)$ :

$$(Vf(\Lambda)V^\dagger)_s \mathbf{w}_i^s = \sigma_i^s \mathbf{w}_i^s \Leftrightarrow V^s f(\Lambda) = W^s \Sigma^s Q^{s\dagger}. \quad (2)$$

Picking more directions on each subdomain than  $n/d$  increases the overlap between the resulting basis  $\mathbf{w}_i$  and the original basis  $\mathbf{v}_i$ , although only  $n$  directions from the over-ranked  $\mathbf{w}_i$  basis are going to be used as the distillation basis,  $W\rho$ , with  $\rho^\dagger\rho = I_n$ , which are the orthogonalization of the projections of  $\mathbf{v}_i$  onto the subspace spanned by  $\mathbf{w}_i$ . In other words,  $\rho$  is the  $Q$ -factor of the QR factorization of  $W^\dagger V$ .

The function  $f$  plays the role of weighing the importance of every direction. To reinforce the presence of the smallest eigenvalues of  $\nabla^2$  into the new basis,  $f$  should be decreasing if we look for the largest singular values of  $V^s f(\Lambda)$ . We have tested a simple family of functions with a single tunable parameter,  $\alpha$ ,  $f(\lambda) = \exp(\alpha\lambda)$ . Figure 1 shows how, as  $\alpha$  increases, the interior eigenvectors get more presence in detriment of the smallest eigenvectors.

When neglecting the perambulators, the hadron correlation functions are reduced to the correlation between baryon elementals at different time-slices. If  $B(\mathbf{v})$  and  $B'(\mathbf{v})$  are two baryon elementals at different time slices, then we want the correlations between  $B(\mathbf{v})$  and  $B'(\mathbf{v})$ , and between  $B(\mathbf{w})$  and  $B'(\mathbf{w})$  to be highly correlated. In this way, we propose the following simple heuristic to tune  $\alpha$  based on the transitive property of correlations for highly correlated data: to maximize the average correlation between the baryon elementals generated with the original basis and with the new basis for a few time-slices. In principle, the correlation between the baryon elementals is not invariant under rotations of the basis, unlike

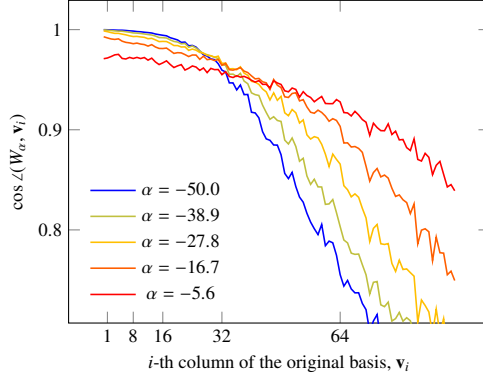


**Figure 1.** Cosine of the angles between each of the columns of the original basis,  $\mathbf{v}_i$ , and the generated basis  $W_\alpha$  with weight function  $f(\lambda) = \exp(\alpha\lambda)$  for different values of  $\alpha$ . The spatial dimension of the lattice is  $32^3$ , blocking 2 in every direction, starting with  $n' = 96$  and picking 128 directions ( $b = 16$ ).

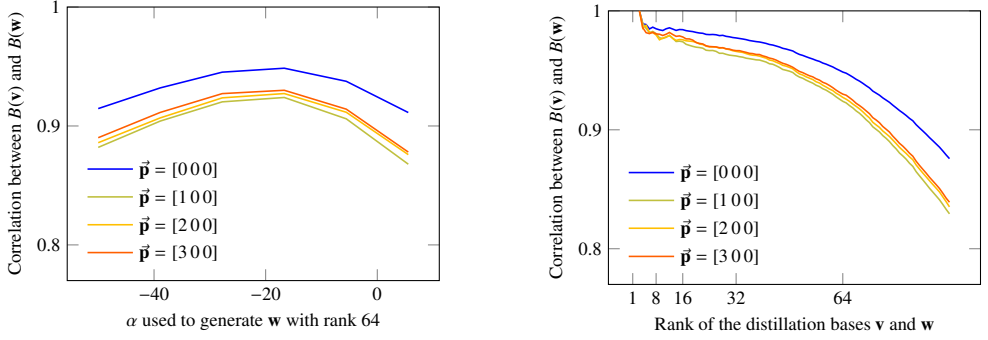


**Figure 2.** Average correlation between the baryon elements generated with the original distillation basis  $\mathbf{v}$  and the blocked basis  $\mathbf{w}$  with weight function  $f(\lambda) = \exp(\alpha\lambda)$ , fixing either both bases rank to 64 (left) or the parameter  $\alpha$  to the optimal value of  $-16.7$  (right). The baryon elements are of the form  $B(\mathbf{v})^{(i,j,k)} = \sum_{\mathbf{x}, \alpha, \beta, \gamma} e^{(\alpha, \beta, \gamma) \cdot \mathbf{v}(\mathbf{x}, \alpha, i)} v^{(\mathbf{x}, \beta, j)} v^{(\mathbf{x}, \gamma, k)} e^{-i(\vec{\mathbf{p}} \cdot \mathbf{x})}$ .

the actual hadron correlation functions. We address this issue in part by selecting  $\rho$  instead so that  $W\rho$  is a close representation of  $\mathbf{v}_i$ ,

$$\rho = \operatorname{argmin}_{\rho^\dagger \rho = I_n} \|V - W\rho\|_F = \hat{U}\hat{\Sigma}\hat{V}^\dagger,$$

where  $\hat{U}\hat{\Sigma}\hat{V}^\dagger$  is the singular value decomposition of  $V^\dagger W$ .

We found that the average correlation function between baryons of both bases is concave and smooth on  $\alpha$ , as Fig. 2 (left) shows. Also, the optimal value of  $\alpha$  seems to depend on neither the momenta nor the displacements of the baryon elemental, and the spectra of  $\nabla^2$  for different time-slices and configurations are similar enough to use the same value of  $\alpha$  for all time-slices. However, we recommend retuning  $\alpha$  when changing the rank of the distillation basis as the correlation quickly drops as the rank increases, as Fig. 2 (right) shows.

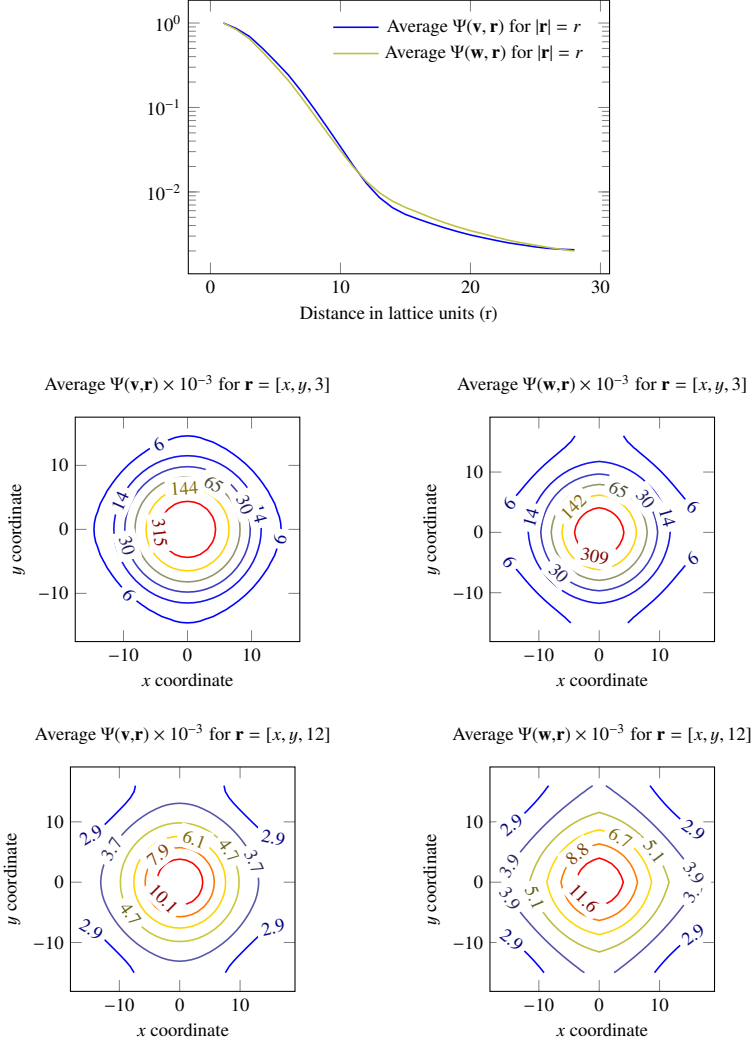


**Figure 3.** Comparison of the spatial distribution of the distillation basis  $\Psi$  of the original basis  $\mathbf{v}$  and the blocked basis  $\mathbf{w}$  in function of the distance (top), and at particular directions (bottom).

Moreover, we tested the spatial distribution of the blocked basis. For that, we study  $\Psi(\mathbf{r})$  as done in [1],

$$\Psi(\mathbf{v}, \mathbf{r}) = \sum_{\mathbf{x} \in L_N} \sqrt{\sum_{\alpha \in C, 1 \leq i \leq n} \mathbf{v}^{(\mathbf{x}, \alpha, i)} \mathbf{v}^{(\mathbf{x} + \mathbf{r}, \alpha, i)^\dagger}}, \quad (3)$$

which measures the degree of smearing on the field after restricting it to the distillation basis. At short distances, both bases seem to keep the rotational symmetry (see Fig 3 top). At long distances, the blocked basis breaks rotational symmetry more than the original basis, as Fig. 3 bottom shows.

Finally, we present the effective masses using the original basis and the blocked basis in Fig. 4 up to momentum 3. Energies computed with both bases are in agreement within statistical error. Thus we do not detect systematic errors introduced by the new basis due to

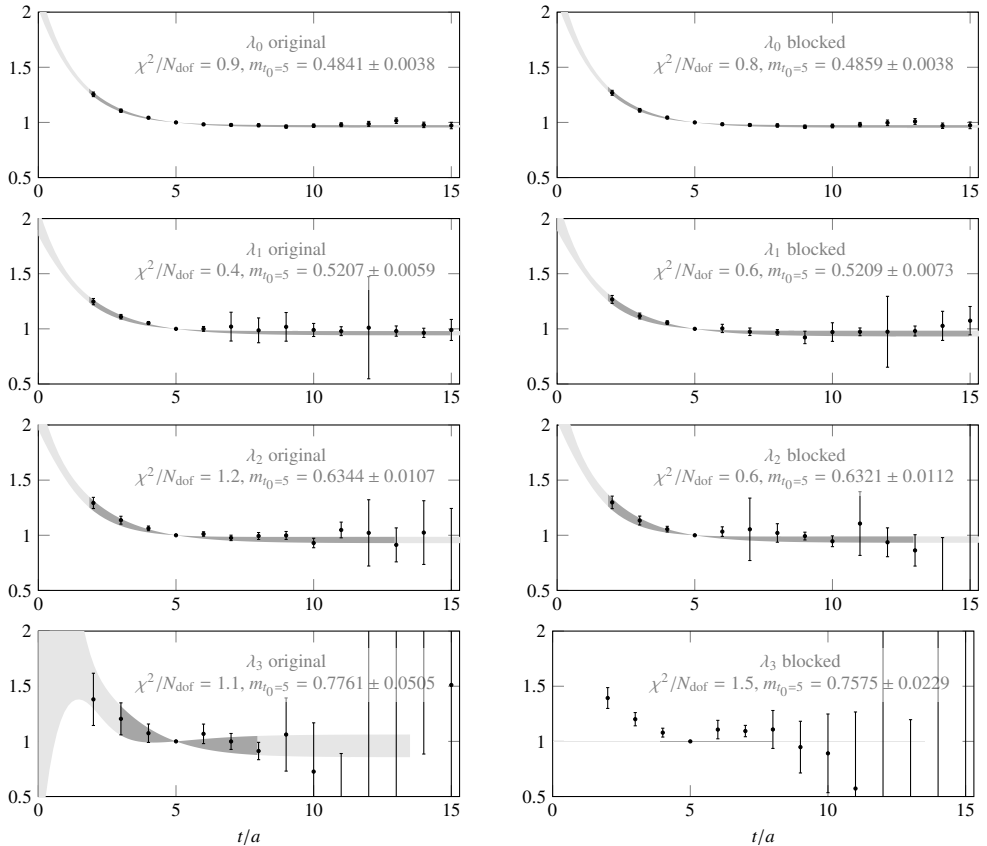


**Figure 4.** Effective masses for time-slice shift of 5 using the original distillation basis (left) and the blocked basis (right) up to momenta 3.

the more pronounced breaking of rotational symmetry. However, the new basis introduces more physical uncertainties in estimating the mass at higher momenta.

To verify the performance benefits, we also developed a prototype code that generates the baryon elementals exploiting the sparsity patterns on the operands of the tensor contraction. The challenge in this development is controlling the overhead of manipulating the sparse representation of tensors. We propose to store the nonzero blocks of the distillation basis and the tensors in a similar way as the Block Sparse Row format does for matrices (see a description at [11]).

It may be still useful to accelerate the contraction of tensors by the BLAS' matrix-matrix multiplication applied to the contraction of the nonzero tensor blocks. Although, some effort is required to reduce the overhead of calling the BLAS function with small matrices. This is especially dramatic for the baryon elementals with displacement, which have a more intricate nonzero pattern of small-size blocks. We got some improvement by static linking with BLAS and choosing the layout of the tensor's matricification carefully to improve data locality. But there is probably still room for improvement. We got a speedup of 2.8 in time, which is far from the expected speedup of 51 if the float-point operations limit the performance. However,

**Table 4.** Expected and measured speedups in the time for computing and writing on the global filesystem the baryon elementals.

Baryon elemental, $B(\mathbf{v})^{(i,j,k)} = \sum_{\mathbf{x}, \alpha, \beta, \gamma} e^{(\alpha, \beta, \gamma)} e^{-i(\vec{\mathbf{p}} \cdot \mathbf{x})} \dots$	Time speedup		Storage reduction	
	Expected	Measured	Expected	Measured
$\dots v^{(\mathbf{x}, \alpha, i)} v^{(\mathbf{x}, \beta, j)} v^{(\mathbf{x}, \gamma, k)}$	64	5.2	8	8
$\dots v^{(\mathbf{x}, \alpha, i)} v^{(\mathbf{x}, \beta, j)} (\mathcal{D}_{\vec{\mathbf{x}}} \mathbf{v})^{(\mathbf{x}, \gamma, k)}$ for $\vec{\mathbf{x}} \in \{\vec{1}, \vec{2}, \vec{3}\}$	50	3.0	4	4
$\dots v^{(\mathbf{x}, \alpha, i)} v^{(\mathbf{x}, \beta, j)} (\mathcal{D}_{\vec{\mathbf{x}}} \mathcal{D}_{\vec{\mathbf{x}}} \mathbf{v})^{(\mathbf{x}, \gamma, k)}$ for $\vec{\mathbf{x}} \in \{\vec{1}, \vec{2}, \vec{3}\}$	50	2.7	4	4
$\dots v^{(\mathbf{x}, \alpha, i)} v^{(\mathbf{x}, \beta, j)} (\mathcal{D}_{\vec{\mathbf{y}}} \mathcal{D}_{\vec{\mathbf{x}}} \mathbf{v})^{(\mathbf{x}, \gamma, k)}$ for $\vec{\mathbf{x}} \neq \vec{\mathbf{y}} \in \{\vec{1}, \vec{2}, \vec{3}\}$	50	2.6	2	2
$\dots v^{(\mathbf{x}, \alpha, i)} (\mathcal{D}_{\vec{\mathbf{x}}} \mathbf{v})^{(\mathbf{x}, \beta, j)} (\mathcal{D}_{\vec{\mathbf{x}}} \mathbf{v})^{(\mathbf{x}, \gamma, k)}$ for $\vec{\mathbf{x}} \in \{\vec{1}, \vec{2}, \vec{3}\}$	50	2.8	2	2
$\dots v^{(\mathbf{x}, \alpha, i)} (\mathcal{D}_{\vec{\mathbf{y}}} \mathbf{v})^{(\mathbf{x}, \beta, j)} (\mathcal{D}_{\vec{\mathbf{x}}} \mathbf{v})^{(\mathbf{x}, \gamma, k)}$ for $\vec{\mathbf{x}} < \vec{\mathbf{y}} \in \{\vec{1}, \vec{2}, \vec{3}\}$	50	2.8	2	2
Average:	51	2.8	3	3

the reduction in the time spent in writing the elementals on the global filesystem is 2.9, as expected. The detailed results are shown on Tab. 4.

## Conclusions

In this work, we propose two techniques to reduce the leading computational costs in estimating baryon correlation functions as the rank of the distillation basis increases, costs that are dominated by the generation and storage of the baryon elementals.

First, we study the performance of generating baryon elementals, which consists of the tensor contraction of the distillation basis, and we propose an implementation that maximizes the CPU utilization. Most of the fine-tuning is avoided by relying on a high-performance BLAS library. Second, we propose to approximate the distillation basis in a spatial local support basis (blocked basis) by exploiting the local coherence of the lattice Laplacian's eigenvectors. The new basis generates very sparse baryon elementals that are more efficient to compute and store, but also contaminates the basis with higher modes that may increase the statistical uncertainty in estimating the correlation functions. Further research will evaluate the effects of the new basis at higher statistical accuracy and on other hadronic states, including excited multihadron states.

Although the asymptotic costs remain the same, the resulting reduction in costs pushes a bit further the practical limits in the lattice volume and the distillation basis' rank employed in these calculations.

## Acknowledgements

This work was primarily supported by the center for nuclear femtography. The gauge field configurations used in this work are from Jefferson Laboratory. The Chroma software suite [12] together with Qphix/mg\_proto [13] and PRIMME [14] have been also used in this work. This work was performed in part using computing facilities at William & Mary which were provided by contributions from the National Science Foundation (MRI grant PHY-1626177), the Commonwealth of Virginia Equipment Trust Fund and the Office of Naval Research. In particular, the majority of this work was performed on the *Femto* cluster at William & Mary.

## References

- [1] M. Peardon, J. Bulava, J. Foley, C. Morningstar, J. Dudek, R.G. Edwards, B. Joó, H.W. Lin, D.G. Richards, K.J. Juge (Hadron Spectrum Collaboration), Phys. Rev. D **80**, 054506 (2009)

- [2] E. Solomonik, D. Matthews, J.R. Hammond, J.F. Stanton, J. Demmel, *Journal of Parallel and Distributed Computing* **74**, 3176 (2014)
- [3] E. Epifanovsky, M. Wormit, T. Kuś, A. Landau, D. Zuev, K. Khistyayev, P. Manohar, I. Kaliman, A. Dreuw, A.I. Krylov, *Journal of Computational Chemistry* **34**, 2293 (2013), <https://onlinelibrary.wiley.com/doi/pdf/10.1002/jcc.23377>
- [4] *William & Mary cluster femto*, <https://www.wm.edu/offices/it/services/hpc/hw/nodes/fe>
- [5] E.D. Napoli, D. Fabregat-Traver, G. Quintana-Ortí, P. Bientinesi, *Applied Mathematics and Computation* **235**, 454 (2014)
- [6] A. Abdelfattah, M. Baboulin, V. Dobrev, J. Dongarra, C. Earl, J. Falcou, A. Haidar, I. Karlin, T. Kolev, I. Masliah et al., *Procedia Computer Science* **80**, 108 (2016), international Conference on Computational Science 2016, ICCS 2016, 6-8 June 2016, San Diego, California, USA
- [7] M. Lüscher, *Journal of High Energy Physics* **2007**, 081 (2007)
- [8] J. Brannick, R.C. Brower, M. Clark, J.C. Osborn, C. Rebbi, *Physical review letters* **100**, 041601 (2008)
- [9] R. Babich, J. Brannick, R.C. Brower, M.A. Clark, T.A. Manteuffel, S.F. McCormick, J.C. Osborn, C. Rebbi, *Phys. Rev. Lett.* **105**, 201602 (2010)
- [10] K. Clark, C. Jung, C. Lehner, *PoS The 35th International Symposium on Lattice Field Theory, LAT2017* (2017)
- [11] Y. Saad, *SPARSKIT: a basic tool kit for sparse matrix computations* (1994)
- [12] R.G. Edwards, B. Joó, *Nuclear Physics B - Proceedings Supplements* **140**, 832–834 (2005)
- [13] B. Joó, D.D. Kalamkar, K. Vaidyanathan, M. Smelyanskiy, K. Pamnany, V.W. Lee, P. Dubey, W. Watson, *Lattice QCD on Intel® Xeon Phi™ Coprocessors*, in *Supercomputing*, edited by J.M. Kunkel, T. Ludwig, H.W. Meuer (Springer Berlin Heidelberg, Berlin, Heidelberg, 2013), pp. 40–54, ISBN 978-3-642-38750-0
- [14] A. Stathopoulos, J.R. McCombs, *ACM Transactions on Mathematical Software* **37**, 21:1 (2010)